第 29 卷第 3 期
2013 年 3 月

无 机 化 学 学 报
CHINESE JOURNAL OF INORGANIC CHEMISTRY

Vol.29 No.3
605-612

$Bi_{3.25}Sm_{0.75}Ti_3O_{12}$ 纳米线的水热合成及可见光催化性能

林 雪*,[1] 关庆丰[2] 邹春杰[1] 刘婷婷[1] 张 瑶[1] 刘春波[1] 翟宏菊[1]
([1]吉林师范大学化学学院,环境友好材料制备与应用教育部重点实验室,四平 136000)
([2]江苏大学材料科学与工程学院,镇江 212013)

摘要: 用一步水热法制备了直径约为 40 nm 的 $Bi_{3.25}Sm_{0.75}Ti_3O_{12}$(BSmT)纳米线。BSmT 纳米线为层状钙钛矿结构。紫外可见漫反射光谱表明,制备出的 BSmT 材料的带隙能约为 2.67 eV。催化反应结果表明,BSmT 的光催化活性比掺氮 TiO_2(N-TiO_2)和纯相钛酸铋($Bi_4Ti_3O_{12}$,BIT)高得多,经可见光照射 360 min,浓度为 0.01 mmol·L^{-1} 甲基橙溶液的降解率可达到 92.0%。BSmT 光催化剂具有更高催化活性的原因是 Sm^{3+}离子掺杂拓展了 BIT 对可见光的吸收范围,同时抑制了 BIT 的光生电子–空穴的复合。并且 BSmT 光催化剂经循环使用 4 次后,其光催化活性并没有明显降低,表明 BSmT 是一种稳定有效的可见光催化剂。

关键词: 钛酸铋; 掺钐; 纳米线; 水热合成; 光催化降解; 可见光照射
中图分类号: O643 **文献标识码**: A **文章编号**: 1001-4861(2013)03-0605-08
DOI: 10.3969/j.issn.1001-4861.2013.00.102

Hydrothermal Synthesis and Visible Light Photocatalytic Property of $Bi_{3.25}Sm_{0.75}Ti_3O_{12}$ Nanowires

LIN Xue*,[1] GUAN Qing-Feng[2] ZOU Chun-Jie[1] LIU Ting-Ting[1]
ZHANG Yao[1] LIU Chun-Bo[1] ZHAI Hong-Ju[1]
([1]*College of Chemistry, Key Laboratory of Preparation and Application of Environmentally Friendly Materials, the Ministry of Education, Jilin Normal University, Siping, Jilin* 136000, *China*)
([2]*School of Materials Science and Engineering, Jiangsu University, Zhenjiang, Jiangsu* 212013, *China*)

Abstract: $Bi_{3.25}Sm_{0.75}Ti_3O_{12}$ (BSmT) nanowires of 40 nm in diameter were synthesized through a one-step hydrothermal process. The BSmT nanowires are of layered perovskites. The results of UV-Visible diffuse reflectance spectra (DRS) demonstrate that the band gap of BSmT nanowires is about 2.67 eV. The BSmT nanowires exhibit higher photocatalytic activity than that of the traditional N doped TiO_2 (N-TiO_2) and pure bismuth titanate ($Bi_4Ti_3O_{12}$, BIT). 92.0% methyl orange (MO) (0.01 mmol·L^{-1}) is decolorized after visible light irradiation for 360 min. The high photocatalytic performance of BSmT photocatalyst could be attributed to the strong visible light absorption and the recombination restraint of the e^-/h^+ pairs resulting from doping of Sm^{3+} ions. In addition, after 4 recycles, there is no significant decrease in the photocatalytic activity, indicating that BSmT is a stable photocatalyst for degradation of MO under visible light irradiation.

Key words: bismuth titanate; samarium doping; nanowires; hydrothermal synthesis; photocatalytic degradation; visible light irradiation

The worldwide quest for clean and renewable energy sources has encouraged a great deal of research activities and development in the field of solar energy in the last twenty years. Therefore, high

收稿日期:2012-10-07。收修改稿日期:2012-11-02。
吉林师范大学博士科研启动项目,环境友好材料制备与应用教育部重点实验室课题资助项目。
*通讯联系人。E-mail:jlsdlinxue@126.com

efficient photocatalyst, photochemical cell, and solar cell have become the hotspot of scientific research. Recently much interest has been devoted to photocatalytic methods, because photocatalysts convert solar energy into clean hydrogen energy by splitting water and decompose harmful organic and inorganic pollutants[1-3]. New and efficient photocatalysts need to be developed besides single component systems such as TiO_2 [4-6]. Recently, it has been reported that bismuth-based oxide semiconductors are potential candidates for highly active photocatalysts, because the Bi6s and O2p levels can form a largely dispersed hybridized valence band[7-8], which favors the mobility of photogenerated holes and is beneficial to the oxidation reaction[9]. Consequently, many efforts have been paid to develop bismuth-containing photocatalysts with high activities for environmental applications and/or water splitting such as $BiVO_4$[10-11], Bi_2WO_6[12-13], BiOBr[14], Bi_2LaTaO_7[15], and $Bi_4Ti_3O_{12}$[16-17], etc. Among bismuth-containing photocatalysts, $Bi_4Ti_3O_{12}$ (BIT) has received more attention for its high photocatalytic ability in degrading the organic pollutants.

In $Bi_4Ti_3O_{12}$-based layered-perovskites, pseudo-perovskite blocks are interleaved with $(Bi_2O_2)^{2+}$ layers along the c-axis and an intra-electric field can be formed between them[18-19]. The bond angle of Ti-O-Ti is about 180°[20-21]. This special structure is beneficial to reducing the recombination of the charge carriers and is helpful for photocatalytic oxidation of organic pollutants, since it might stimulate the separation of electron-hole pairs and facilitate the mobility of photogenerated carriers to the surface of the crystals. It is, therefore, of interest to study the photocatalytic activity of BIT crystals. Photocatalytic properties of BIT have been examined before. Kudo et al. [22] reported the preparation of BIT prepared by the solidsolid method and examined the photocatalytic activity of BIT for water splitting. Recently, Yao et al.[17] investigated the photocatalytic activity of BIT fabricated by using the chemical solution decomposition (CSD) method. In our previous work, we presented the hydrothermal synthesis of BIT microspheres and tested the photocatalytic properties of the as-prepared BIT microspheres[23].

In order to maximize the photocatalysis efficiency, it is very important to minimize the recombination rate. It is known that metal ions doped into catalysts can increase the quantum efficiency of the heterogeneous photocatalytic property by altering the e^-/h^+ pair recombination rate and promoting the interfacial charge transfer rates of photogenerated carriers [24-26]. Therefore, Metal elements doping is one of the typical approaches to extend the spectral response of BIT photocatalysts by providing defect states in the band gap [27-28]. So it is of interest to investigate the influence of metal doping on the photocatalytic property of BIT. However, to our knowledge, few papers have revealed the photocatalytic activity of samarium doped bismuth titanate ($Bi_{3.25}Sm_{0.75}Ti_3O_{12}$, BSmT) crystals for oxidizing organic contaminants in water. The activity of photocatalysts is influenced by a wide variety of factors such as, the catalysts preparation conditions, crystal morphology, the adsorption affinity and capacity for organic contaminants, pH value, intrinsic solid state defects and so on. The aim of the present work is to study the influence of Sm-doping on the microstructure, optical properties and photocatalytic properties of BIT photocatalysts.

1 Experimental

1.1 Preparation of BSmT photocatalysts

All the chemicals were analytically grade (purchased from Shanghai chemical Industrial Company) and used without further purification. BSmT samples were prepared with a one-step hydrothermal synthesis. Bismuth nitrate ($Bi(NO_3)_3\cdot 5H_2O$), Samarium nitrate ($Sm(NO_3)_3\cdot 6H_2O$) and titanium tetrachloride ($TiCl_4$) were chosen as starting materials with the molar ratio of bismuth:lanthanum:titanium ions (3.25:0.75:3.00). 10 mL of $TiCl_4$ was dissolved in cold water (50 mL) under vigorous stirring, then mixed with $Bi(NO_3)_3\cdot 5H_2O$ and $Sm(NO_3)_3\cdot 6H_2O$. The concentration of the alkali solution was adjusted using KOH. Before being transferred to a 20 mL stainless steel autoclave,

the solution mixture was prepared under an ultrasonic water bath for 30 min and kept at a filling ratio of 70% (volume fraction). The autoclave was kept at 180 ℃ for 24 h, and cooled to room temperature after the reaction. The precipitates were washed with deionized water and ethanol three times, separately. The final products were dried at 100 ℃ for 2 h in a vacuum box. The samples prepared for comparison were (i) BIT and (ii) N doped TiO_2 (N-TiO_2). For more details about the preparation of BIT and N-TiO_2, the readers can refer to our previous work[29-30].

1.2 Characterization of photocatalysts

The crystal structures of the samples were characterized by X-ray diffraction (XRD) on a Rigaku (Japan)D/max 2500 X-ray diffractometer (Cu $K\alpha$ radiation, λ=0.154 18 nm), employing a scanning rate of 4.00°·min^{-1}, in the 2θ range from 20° to 50°. Transmission electron microscopy (TEM) was conducted using a JEM-2100F (Japan JEOL) instrument at accelerating voltage of 200 kV. The chemical composition of the compound was determined by scanning electron microscope-X-ray energy dispersion spectrum (SEM-EDX). The infrared (IR) spectra were measured by infrared spectrometer (America Perkin Elmer, Spectrum One). The UV-Vis diffuse reflectance spectra (DRS) were recorded for the dry-pressed disk sample using a scan UV-Vis spectrophotometer (UV-Vis, Japan SHIMADZU, UV-2550) equipped with an integrating sphere assembly.

1.3 Photocatalytic activity test

The photocatalytic degradation of methyl orange (MO) was employed to evaluate the photocatalytic activity of the samples. A 300 W Xe lamp (λ>420 nm) was used to provide visible light irradiation. 0.10 g of photocatalyst was added to 100 mL of MO solution (0.01 mmol·L^{-1}). Before irradiation, the suspensions were magnetically stirred in the dark for 30 min to ensure the adsorption-desorption equilibrium between the photocatalysts and MO. Then the solution was exposed to visible light irradiation under magnetic stirring. At given time intervals, 4 mL of suspension was sampled and centrifuged to remove the photocatalyst particles. Then, the catalyst-free dye solution was analyzed by a UV-2550 spectrometer to record intensity of the maximum band at 462 nm in the UV-Vis absorption spectra.

2 Results and discussion

2.1 XRD analysis

Fig.1 shows XRD patterns of the as-prepared BSmT products synthesized at OH^- concentrations of 3 mol·L^{-1} and 8 mol·L^{-1}, respectively. All the reflection peaks can be indexed according to the PDF No. 36-1486, suggesting that the as-prepared products are of layered-perovskite structure ($Bi_4Ti_3O_{12}$). No peaks of impurities were detected from the patterns. The strong and sharp peaks indicate high crystallinities of BSmT samples.

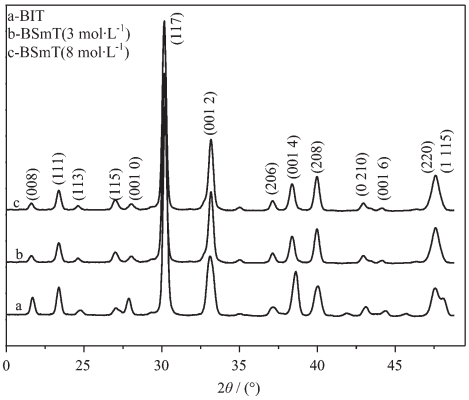

T=180 ℃, t=24 h

Fig.1 XRD patterns of samples BIT and BSmT

2.2 IR analysis

IR spectra of BIT and BSmT are shown in Fig.2. It can be seen that there are two strong absorption

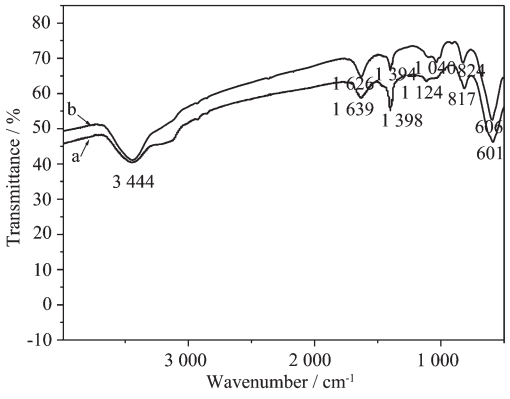

T=180 ℃, t=24 h

Fig.2 IR spectra of the samples BIT (a) and BSmT (b)

bands at 817 cm^{-1} and 601 cm^{-1} in the IR spectrum of BIT (Fig.2). Based on the study of Pinheiro et al.[31], the two absorption bands belong to the stretching vibration of the Ti-O bond. The IR spectrum of BSmT is similar with that of BIT except for the difference in the locations of the absorption bands. The absorption peaks at 817 cm^{-1} and 601 cm^{-1} show red shift of 7 cm^{-1} and 5 cm^{-1}, respectively. That may be associated with the substitution of Bi^{3+} ions in BIT crystal by Sm^{3+}.

2.3 TEM analysis

Fig.3 (a) shows the TEM images of the BSmT sample synthesized at OH^- concentration of 3 $mol \cdot L^{-1}$. It can be observed that BSmT products are composed of nano-sized particles. The average size of BSmT crystals is 25 nm (as shown in Fig.3(b)). Fig.3(c) gives TEM image of the BSmT sample obtained at OH^- concentration of 8 $mol \cdot L^{-1}$. It can be seen that there are BSmT nanowires with width of approximately 40 nm and lengths up to several micrometres. Further structure details of BSmT nanowires are illustrated in Fig.3 (d). It reveals that some small nanoparticles could also be observed in the sample prepared at OH^- concentration of 8 $mol \cdot L^{-1}$. These results show that OH^- concentration seems to play a key role in controlling the morphologies of BSmT crystals.

Although the crystal growth habit is mainly determined by the intrinsic structure, it is also affected by the external conditions such as the pH value of the solution, saturation, temperature and so on [32]. OH^- concentration in the precursor solution is very important for the microstructure. In this work, the condition of the alkaline medium as a factor is considered to play an important part in the formation of BSmT nanowires. At lower OH^- concentration (3 $mol \cdot L^{-1}$), BSmT nuclei produced in solution can aggregate to form small particles. These particles may serve as crystal seeds to grow the nanowires structure. With the increase of alkalinity (OH^- concentration: 8 $mol \cdot L^{-1}$), a large amount of BSmT nuclei is produced in the solution, leading to the formation of a very high supersaturation solution, which favors the formation of nanowires structure. Hence, the formation of BSmT nanowires in the present route is resulted from the highly alkaline medium.

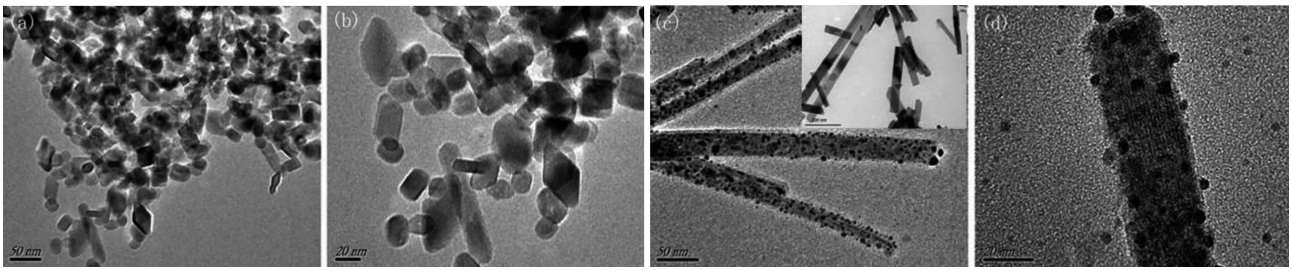

(a, b): C_{OH^-}=3 $mol \cdot L^{-1}$, (c, d): C_{OH^-} =8 $mol \cdot L^{-1}$, Inset: TEM images of pure BIT sample

Fig.3 TEM images of BSmT samples (T=180 ℃, t=24 h) obtained at different concentrations of OH^-

HRTEM image is shown in Fig.4 to reveal the detailed crystal structure of the as-prepared BSmT nanowires. The lattice distance for BSmT sample is calculated to be 0.38 nm, which is in agreement with th (111) lattice plane of the layered-perovskite BIT. Thus, we can conclude that the low concentration doping of Sm^{3+} ions does not induce the formation of separated pure phases (samarium metal).

Fig.5 shows EDX results of BSmT composite, the molar ratios of Bi/Ti and Bi/Sm are calculated to be 1.09 and 4.74, respectively, which are in accordance with the nominal molar ratio of $Bi_{3.25}Sm_{0.75}Ti_3O_{12}$.

2.4 UV-Vis DRS spectral analysis

The UV-Vis DRS of the as-prepared BSmT nanowires is shown in Fig.6. The absorption onset wavelength λ_g of BSmT nanowires is around 465 nm, which is shifted 39 nm to visible region compared to pure BIT sample. The band gap of BSmT was calculated to be 2.67 eV, based on the formula: E_g(eV) =1 240/λ_g (nm). Interestingly, three absorption bands appear in the visible region above 500 nm in the

T=180 ℃, t=24 h, C_{OH^-}=8 mol·L^{-1}

Fig.4　HRTEM image of BSmT nanowires

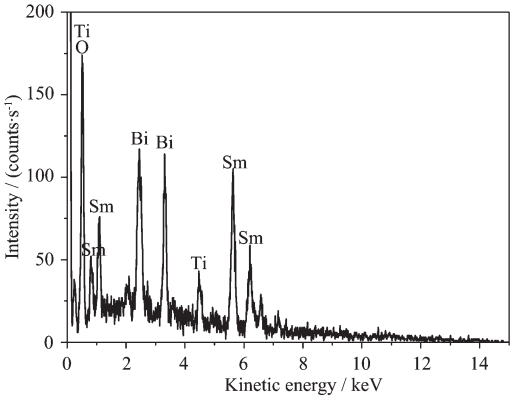

T=180 ℃, t=24 h, C_{OH^-}=8 mol·L^{-1}

Fig.5　EDX spectrum of the as-prepared BSmT nanowires

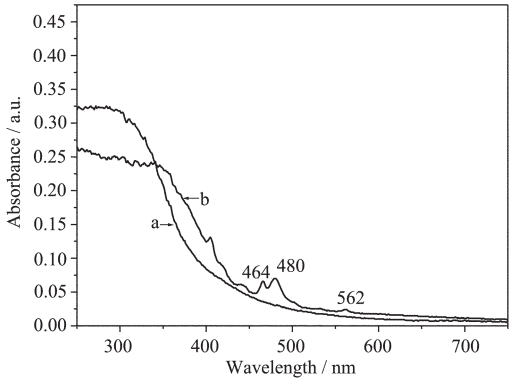

T=230 ℃, t=24 h, C_{OH^-}=8 mol·L^{-1}

Fig.6　UV-Vis DRS of BIT (a) and BSmT (b)

absorption spectrum shown in Fig.6. They are attributed to the absorption of Sm^{3+} since no any absorption band was detected in the visible region for BIT.

2.5　Degradation of MO using BSmT photocatalysts

The photocatalytic activity of the as-prepared BSmT nanowires was evaluated by the degradation of MO solution. For comparison, the photodegradation of MO by N-doped TiO_2, pure BIT, and that without any catalyst were also carried out. Temporal courses of the photodegradation of MO in different catalyst aqueous dispersions are shown in Fig.7 (a) while the corresponding UV-Vis spectral changes of these solutions are displayed in the inset. The result shows that the absorption peak corresponding to the MO molecules at 462 nm rapidly decreases in intensity with exposure time. It also can be observed that MO solution is stable under visible light irradiation in the absence of any catalyst. When BSmT nanowires has been added to the MO solution, the total degradation rate is over 92.0% within 360 min irradiation, much higher than that of N-TiO_2 which only reaches 52.0% of the total decomposition. Thus, the addition of BSmT photocatalyst leads to the obvious degradation of MO. In comparison, the photocatalytic degradation rate of MO over BIT is about 80.0%, approximately.

To quantitatively study the photocatalytic reaction kinetics of the MO degradation in the experiments, the degradation data is analyzed with the pseudo-first-order model, as expressed by Eq.(**1**)[33]:

$$\ln(C_0/C) = kt \quad (1)$$

where C_0 and C represent MO concentration at time zero and t, respectively, and k is the pseudo first-order rate constant. The first-order linear relationship is revealed by the plots of the $\ln(C/C_0)$ vs irradiation time (t), as shown in Fig.7(b). The reaction rate constant k for MO, N-TiO_2, BIT and BSmT are 0.000 226, 0.001 99, 0.004 01, and 0.007 02 min^{-1}, respectively, indicating the highest photocatalytic performance of BSmT nanowires. Based on the above analysis, it can be concluded that Sm doping can significantly improve the performance of BIT photocatalysts.

BSmT samples reveal high photocatalytic activity with the MO degradation efficiency of 85.0%, 88.0%, and 92.0%, respectively, as the doping amount of Sm^{3+}

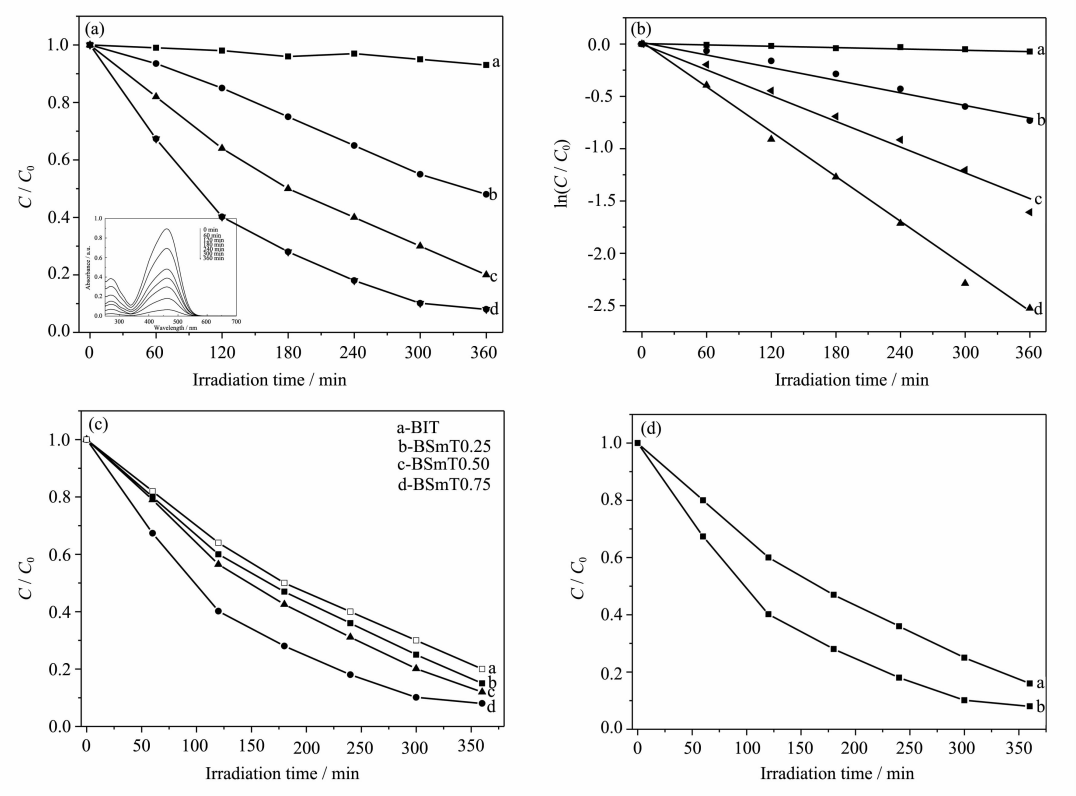

Fig.7 (a) Temporal courses of the photodegradation of MO in different catalyst aqueous dispersions. The inset is the corresponding UV-Vis spectral changes of MO by BSmT sample

(b) First-order plots for the photocatalytic degradation of MO using different catalysts: (a) without catalyst, (b) N-TiO_2, (c) BIT, (d) BSmT

(c) Temporal courses of the photodegradation of MO in different catalyst aqueous dispersions

(d) Temporal courses of the photodegradation of MO in BSmT sampes prepared at different concentrations of OH^-: (a) C_{OH^-}=3 mol·L^{-1}, (b) C_{OH^-}=8 mol·L^{-1}

increases (Fig.7(c)). Obviously, BSmT0.75 exhibits the highest photocatalytic degradation efficiency among those samples. Based on the above analysis, it can be concluded that Sm doping is one of the typical approaches to improve the performance of BIT photocatalysts. Temporal course of the photodegradation of MO by BSmT samples prepared at different OH^- concentrations is shown in Fig.7(d). It can be seen that BSmT nanowires prepared at OH^- concentration of 8 mol·L^{-1} show relatively higher photocatalytic degradation efficiency. This result shows that the performance of BSmT nanowires is better.

2.6 Stability of BSmT as the photocatalyst

Fig.8 shows the XRD patterns of the BSmT sample after 360 min of visible light irradiation. It can be seen that both the position and the intensity of the peaks in the XRD pattern are almost the same as those of BSmT before irradiation. Thus, BSmT

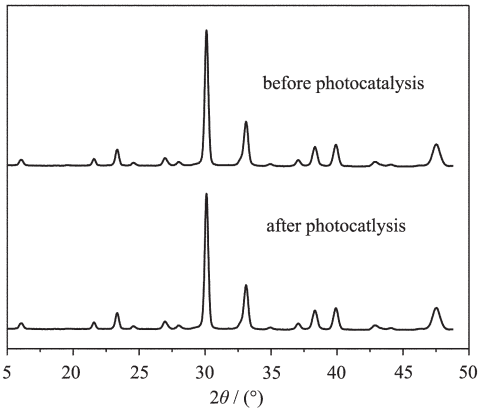

Fig.8 XRD patterns of BSmT before and after visible light irradiation

photocatalyst is considered to be relatively stable to visible light irradiation under the present experimental conditions. This result indicates a possibility for application of BSmT photocatalyst in the waste water treatment.

The stability tests results by using recycling reactions four times for the photodegradation of MO over BSmT photocatalyst under visible light irradiation are displayed in Fig.9. No significant decrease in catalytic activity is detected in the recycling reactions. Combined with the XRD patterns, all evidences demonstrate that the BSmT photocatalyst is a stable photocatalyst for degradation of MO under visible light irradiation.

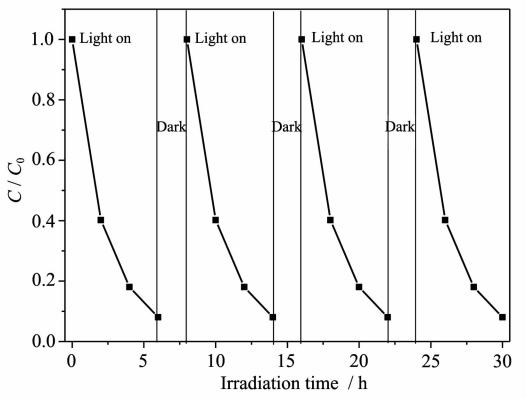

Fig.9　Stability evaluation for BSmT: four reaction cycles for photodegradation of MO under visible light irradiation

2.7　Photocatalytic activity mechanism

On the basis of our previous work[29-30], a schematic diagram of the band levels of doped BIT and the possible reaction mechanism of the photocatalytic procedure are proposed and illustrated. The possible photocatalytic mechanism of BSmT is established and a schematic diagram is shown in Fig.10.

As calculated by Goto et al[34], the CB and VB of Nd doped bismuth titanate (BNdT) consist mostly of empty Ti3*d* and occupied O2*p* orbitals, respectively, and the latter is hybridized with Bi6*s* and Nd5*d*. These bands meet the potential requirements of organic oxidation. Therefore, in the present hybridized VB composed of O2*p* and Bi6*s*, the photogenerated carriers may own a high mobility. Then it will reduce the recombination opportunities of the photogenerated

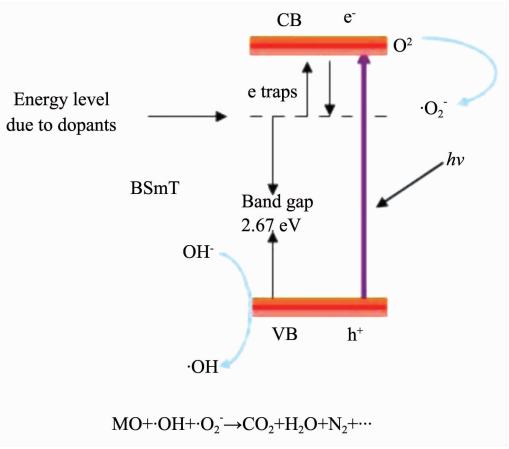

Fig.10　Schematic diagram of photocatalytic mechanism for BSmT nanowires

electron-hole pairs that could effectively move to the crystal surface to degrade the absorbed MO molecule. Based on the above consideration, we presume that the CB and VB of BSmT consist mostly of empty Ti3*d* and occupied O2*p* orbitals, respectively, and the latter is hybridized with Bi6*s* and Sm5*d*.

In a typical photodegradation of organic pollutants process, when the semiconductor is irradiated by light, the photoexcited electrons can be transferred to the conduction band (CB) from the valence band (VB) and whilst the holes form in the VB. Then the photoexcited holes in the VB can form ·OH (hydroxyl radical) that can oxidize the organic pollutants and the electrons in the CB participate in the reduction process. Thus, Sm doping would result in the improvement of the corresponding photocatalytic properties, as clarified by following equations:

$$BSnT+h\nu \rightarrow BSmT(e^-+h^+) \quad (2)$$

$$H_2O \rightarrow H^++OH^- \xrightarrow{h^+} \cdot OH \quad (3)$$

$$O_2 \xrightarrow{e^-} \cdot O_2^- \quad (4)$$

$$MO+\cdot OH+\cdot O_2^- \rightarrow CO_2+H_2O+N_2+\cdots \quad (5)$$

Thus, the higher photocatalytic activity of BSmT over TiO_2 and BIT is attributed to suitable band gap and stable e-h pair formation in the VB formed by the hybrid orbitals of Bi6*s*, Sm5*d* and O2*p* and the CB of Ti3*d*.

3　Conclusions

$Bi_{3.25}Sm_{0.75}Ti_3O_{12}$ nanowires were synthesized by a

one-step hydrothermal process without the use of any surfactants or templates. The optical band gap of BSmT nanowires is estimated to be about 2.67 eV, which proves that BSmT photocatalysts can respond to the visible light. Most importantly, BSmT photocatalysts with good stability exhibits higher photocatalytic performance in the degradation of methyl orange under visible light irradiation (λ>420 nm) than that of traditional N doped TiO_2, and pure BIT. Over this catalyst, a 92.0% degradation of MO solution (0.01 mmol·L^{-1}) is obtained after visible light irradiation for 360 min. In addition, after 4 recycles, there is no significant decrease in the photocatalytic activity, indicating that BSmT is a stable photocatalyst for degradation of MO under visible light irradiation.

References:

[1] Wang S L, Li P G, Zhu H W, et al. *Powder Technol.*, **2012**, **230**:48-53

[2] YU Chang-Lin(余长林), ZHOU Wan-Qin(周晚琴), YU Jimmy C. *Chinese J. Inorg. Chem.* (*Wuji Huaxue Xuebao*), **2011**,**27** (10):2033-2038

[3] LI Yue-Jun(李跃军), CAO Tie-Ping(曹铁平), WANG Chang-Hua(王长华), et al. *Chinese J. Inorg. Chem.* (*Wuji Huaxue Xuebao*), **2011**,**27**(10):1975-1980

[4] YAN Ya(严亚), LV Ying(吕瑛), XIA Yi(夏怡), et al. *Chinese J. Inorg. Chem.* (*Wuji Huaxue Xuebao*), **2011**,**27** (10):1999-**2004**.

[5] Ghaffari M, Huang H, Tan P Y, et al. *Powder Technol.*, **2012**, **225**:221-226

[6] Uyguner-Demirel C S, Bekbolet M. *Chemosphere*, **2011**,**84**: 1009-1031

[7] Xu J J, Chen M D, Fu D G. *Appl. Surf. Sci.*, **2011**,**257**:7381-7386

[8] Xu J, Wang W Z, Shang M, et al. *J. Hazard Mater.*, **2011**,**196**: 426-430

[9] Yao W F, Wang H, Xu X H, et al. *Appl. Catal. A*: *Gen.*, **2004**, **259**:29-33

[10]Yu J Q, Zhang Y, Kudo A. *J. Solid State Chem.*, **2009**,**182**: 223-228

[11]Li J Q, Wang D F, Liu H, et al. *Phys. Status Solidi A*, **2012**, **209**:248-253

[12]Zhang L W, Wang Y J, Cheng H Y, et al. *Adv. Mater.*, **2009**, **21**:1286-1290

[13]Zhang L S, Wang H L, Chen Z G, et al. *Appl. Catal. B*: *Environ.*, **2011**,**106**:1-13

[14]Zhang L, Cao X F, Chen X T, et al. *J. Colloid Interf. Sci.*, **2011**,**354**:630-636

[15]Luan J F, Hao X P, Zheng S R, et al. *J. Mater. Sci.*, **2006**,**41**: 8001-8012

[16]Yao W F, Xu X H, Wang H, et al. *Appl. Catal. B*: *Environ.*, **2004**,**52**:109-116

[17]Yao W F, Wang H, Xu X H, et al. *Mater. Lett.*, **2003**,**57**:1899-1902

[18]Buscaglia M T, Sennour M, Buscaglia V, et al. *Cryst. Growth Des.*, **2011**,**11**:1394-1401

[19]Chen X H, J Q Hu, Chen Z W, et al. *Biosens. Bioelectron.*, **2009**,**24**:3448-3454

[20]Chen Z W, He X H. *J. Alloys Compd.*, **2010**,**497**:312-315

[21]Patwardhan J S, Rahaman M N. *J. Mater. Sci.*, **2004**,**39**:133-139

[22]Kudo A, Hijii S. *Chem. Lett.*, **1999**,**28**:1103-1104

[23]Lin X, Lv P, Guan Q F, et al. *Appl. Surf. Sci.*, **2012**,**258**: 7146-7153

[24]Ghorai T K, Biswas S K, Pramanik P. *Appl. Surf. Sci.*, **2008**, **254**:7498-7504

[25]Castro A L, Nunes M R, Carvalho M D, et al. *J. Solid State Chem.*, **2009**,**182**:1838-1845

[26]Tang X D, Ye H Q, Zhao Z, et al. *Catal. Lett.*, **2009**,**133**:362-369

[27]Yao W F, Wang H, Shang S X, et al. *J. Mol. Catal. A*: *Chem.*, **2003**,**198**:343-348

[28]Wang Z Z, Qi Y J, Qi H Y, et al. *J. Mater. Sci.*: *Mater. Electron.*, **2010**,**21**:523-528

[29]LIN Xue(林雪), GUAN Qing-Feng (关庆丰), LI Hai-Bo (李海波), et al. *Acta Phys.-Chim. Sin.* (*Wuli Huaxue Xuebao*), **2012**,**28**:1481-1488

[30]LIN Xue(林雪), LV Peng(吕鹏), GUAN Qing-Feng (关庆丰), et al. *Acta Phys.-Chim. Sin.* (*Wuli Huaxue Xuebao*), **2012**,**28**: 1978-1984

[31]Pinheiro A G, Pereira F M M, Santos M R P, et al. *J. Mater. Sci.*, **2007**,**42**:2112-2120

[32]Yang J H, Zheng J H, Zhai H J, et al. *J. Alloys Compd.*, **2009**,**481**:628-631

[33]Tauc J. *Amorphous and Liquid Semiconductors*. New York: Plenum Press, **1974**:159

[34]Goto T, Noguchi Y, Soga M, et al. *Mater. Res. Bull.*, **2005**,**40**: 1044-1051